tions to conclude that at least two types of recombination centre are involved. At n-type GaP electrodes recombination occurs not only at the surface, but also deeper in the solid. An analysis of the recombination impedance shows that, besides surface recombination, recombination in the depletion layer must be taken into account.

References

[1] D. Vanmaekelbergh, W. P. Gomes, and F. Cardon, Ber. Bunsenges. Phys. Chem. *90*, 431 (1986).
[2] J. E. A. M. van den Meerakker, J. J. Kelly, and P. H. L. Notten, J. Electrochem. Soc. *132*, 638 (1985).
[3] K. Schröder and R. Memming, Ber. Bunsenges. Phys. Chem. *89*, 385 (1985).
[4] B. Wolf and W. Lorenz, Electrochim. Acta *28*, 699 (1983).
[5] P. Allongue and H. Cachet, J. Electrochem. Soc. *132*, 45 (1985).
[6] D. Vanmaekelbergh, W. P. Gomes, and F. Cardon, Ber. Bunsenges. Phys. Chem. *89*, 994 (1985).
[7] D. Vanmaekelbergh, W. P. Gomes, and F. Cardon, J. Electrochem. Soc. *134*, 891 (1987).
[8] D. Vanmaekelbergh and F. Cardon, J. Phys. D: Appl. Phys. *19*, 643 (1986).
[9] D. Vanmaekelbergh and F. Cardon, Semicond. Sci. Technol. *3*, 124 (1988).
[10] D. Vanmaekelbergh, J. J. Kelly, S. Lingier, and W. P. Gomes, Ber. Bunsenges. Phys. Chem. *92*, 1068 (1988).
[11] D. Vanmaekelbergh and J. J. Kelly, J. Electrochem. Soc. *136*, 108 (1989).
[12] P. Allongue and H. Cachet, Ber. Bunsenges. Phys. Chem. *91*, 386 (1987).
[13] J. Li and L. M. Peter, J. Electroanal. Chem. *199*, 1 (1986).
[14] D. Vanmaekelbergh, W. P. Gomes, and F. Cardon, Ber. Bunsenges. Phys. Chem. *89*, 987 (1985).
[15] K. H. Beckmann and R. Memming, J. Electrochem. Soc. *116*, 368 (1969).
[16] B. Smandek and H. Gerischer, Electrochim. Acta *30*, 1101 (1985).
[17] Y. Nakato, K. Morita, and H. Tsubomura, J. Phys. Chem. *90*, 2718 (1986).
[18] J. Li, R. Peat, and L. M. Peter, J. Electroanal. Chem. *165*, 41 (1984).

(Eingegangen am 3. Juli 1989, E 7132
endgültige Fassung am 27. Juli 1989)

Polycrystalline Boron Phosphide Semiconductor Electrodes

A. Goossens, E. M. Kelder, and J. Schoonman

Delft University of Technology, Laboratory for Inorganic Chemistry, Julianalaan 136, 2628 BL Delft, The Netherlands

Electrochemistry / Interfaces / Semiconductors / Spectroscopy, Impedance

Thin films of polycrystalline boron phosphide (BP) are obtained by using conventional thermally activated chemical vapor deposition. BBr_3 and PBr_3 are used as reactants and BP is formed at 940°C in a H_2 environment. A rough black layer is obtained on alumina substrates. All films are n-type with a high donor density. (Photo-) current-voltage curves are presented. The transient photocurrent response and the presence of a substantial photocurrent at subbandgap illumination strongly suggests the presence of a high density of surface states. Impedance spectra of the unilluminated electrode could be modelled adequately with an equivalent circuit. Numerical values of the space charge capacitance were obtained at anodic potentials. The flatband potential was determined from Mott-Schottky plots, and appeared to depend strongly on the electrolyte pH. The flatband potential of BP is (+0.182 − 0.073 pH) V vs. SHE. This value is not concordant with reported theoretical predictions based on atomic electronegativities.

Introduction

Boron monophosphide (BP) exhibits a variety of interesting material characteristics that may be applied in a broad spectrum of practical applications. BP is a covalent 111-V compound with the cubic zincblende structure. The material is thermally stable up to high temperatures, and resists corrosion in extreme environments. BP is a semiconductor with an indirect bandgap of about 2 eV [1]. These material characteristics make BP an interesting candidate for photoelectrochemical applications. Usually BP is grown by Chemical Vapor Deposition (CVD) techniques. In spite of the large difference between the lattice constant of Si and BP, boron phosphide can be grown epitaxially on Si substrates [2].

Takenaka et al. [3] suggested the utilization of a thin BP layer as optical window for Si solar cells. In particular, epitaxial BP coatings were used in the Schottky-barrier heterojunctions Si/BP and GaAs/BP, which have been studied as photo-anodes in regenerative photo-electrochemical (PEC) cells [4]. Epitaxial BP coatings were reported to successfully protect Si and GaAs against photocorrosion.

The band structure of these heterojunctions has been derived using a value of −0.5 V vs. SHE for the flatband potential of BP [4]. This value has been determined empirically by Butler and Ginley [5] from atomic electronegativities. The flatband potential has not yet been determined experimentally. Neither have the Schottky-barrier heterofunctions been characterized electrochemically.

In the CVD of BP films on Si and GaAs, interface reactions can not been excluded. Solid-gas reactions before deposition may affect charge densities in the substrates and enhance the presence of surface states which could destroy the photoelectrochemical properties at the junction.

We have studied CVD films of polycrystalline BP by impedance spectroscopy in order to determine the flatband potential. In polycrystalline electrodes Mott-Schottky plots are often found to be nonlinear and frequency dependent. If, however, interfacial capacitances are obtained from an analysis of impedance spectra, frequency invariant and, in our case, linear Mott-Schottky plots are obtained and hence the flatband potential, and the Mott-Schottky slope can be determined unambiguously. In this paper we report on the impedance characteristics of BP/electrolyte heterojunctions.

In addition, current-voltage characteristics have been studied. Upon irradiation substantial recombination effects occur. Transient photocurrent behavior with chopped illu-

mination indicates the presence of electron states within the bandgap at the boron phosphide surface.

Experimental Aspects

Polycrystalline films of BP were deposited on alumina substrates by thermally activated atmospheric pressure Chemical Vapor Deposition (CVD). Boron tribromide and phosphorus tribromide were used as reactants. Hydrogen purified with a palladium catalyst and dried by 4A zeolite was bubbled through the reactants with a constant controlled flow rate and brought to a well defined temperature in heat exchange zones. Temperatures are chosen as to make the partial pressure of both vapors equal. These temperatures were 3.5°C for BBr_3 and 64°C for PBr_3 and were stabilized to an accuracy of 0.1°C. Hereafter the reactant vapors were diluted with H_2 to a fraction of 5% and led into the furnace. The concentration ratio $[BBr_3]$: $\{[BBr_3] + [PBr_3]\}$ was 1:6 and the H_2 bulk flow was about 200 l/h. The furnace and substrate temperature were 940°C and the deposition time was 20 min. Subsequently the samples were thermally annealed in hydrogen for 30 min. at 900°C. A horizontal quartz tube reactor (ID 4 cm) was used in which tilted samples were mounted on a quartz sample holder. The substrates were preheated in air at 1100°C in order to remove organic detergents.

The crystal structure of the material was studied by XRD. Auger analyses provided information on the stoichiometry of the B_xP deposits. Surfaces of the CVD films were studied with scanning electron microscopy SEM (JEOL JSM-35).

To determine the resistivity and the Hall coefficient with the Van der Pauw method four ohmic copper contacts were provided on the corners of the rectangular samples. The resistivity and Hall coefficient were determined at room temperature. An electrical current of 100 μA was applied. The potential differences were recorded with a Keithley 150B Microvolt ammeter. For determination of the Hall coefficient a Varian magnet V 3603, with magnetic field strengths ranging from 0.1 to 1.0 Tesla was used. Because the measuring current slowly heated the sample, which was manifest in a continuous variation in the Hall potential, the system was stabilized for several hours before performing a measurement.

The sample was mounted in a photoelectrochemical (PEC) cell provided with a Pt counter electrode, and a saturated calomel reference electrode (SCE). In order to prevent contamination of the electrolyte with KCl, the SCE was placed in a saturated KCl solution which was connected to a container with electrolyte which in turn was bridged to the electrolyte in the PEC cell. The four Cu contacts on the surface served as working electrode contact. As electrolytes: [1]: H_2SO_4 (0.1 M), [2]: H_2SO_4 (0.05 M) + KCl (1 M), [3]: KOH (0.1 M), [4]: HAc (0.05 M) + NaAc (0.05 M) + KCL (1 M), and [5]: $Na_2B_4O_7$ (0.1 M) + KCl (1 M) were used. The BP/electrolyte geometrical contact surface area was in all cases 0.2 cm^2.

Current-voltage curves were obtained in the dark, and upon illumination by slowly sweeping the potential, <1 mV/s. The radiation source used was a 450 W high pressure Xenon lamp with IR filtering. Transient $i-V$ curves were recorded using chopped illumination with a similar potential sweep. The chop rate could be varied between 40 mHz and 10 Hz. A sequence of Schott high pass filter glasses together with a UV cut-off filter were used in order to record the spectral photocurrent. The anodic potential was kept constant at 1.2 V vs. SCE and stable photocurrents corrected for dark-currents are determined.

Impedance spectra of uniradiated PEC cells were recorded. The frequency range applied was 10^{-1} to 10^5 Hz with an a.c. potential amplitude of 20 mV. A Solartron (1250) Frequency Response Analyzer coupled to a Solartron (1286) Electrochemical Interface was used. The a.c. potential was superimposed on a d.c. polarization potential. The system was stabilized before the frequency sweep was applied.

Results

Polycrystalline boron phosphide deposits on alumina substrates have a black appearance. The coatings are homogeneous over the entire substrate surface. The deposit adheres extremely well to the alumina substrate. The deposition rate obtained is typically about 10 μm per hour. The samples used in this paper all have a thickness of about 5 μm.

From X-ray diffraction measurements the zincblende structure of polycrystalline BP could be confirmed unambiguously.

From Auger analyses the boron to phosphor ratio (x) in B_xP was determined to be about one. Besides B and P, no other elements except some adsorbed oxygen and carbon are found at the surface.

Scanning Electron micrographs reveal a substantial surface roughness. The surface can best be described as a collection of BP spherical like crystallites with radii of typically 2–3 μm, stacked in a completely random way. It seems very well plausible that the actual surface area could be an order of magnitude greater than the geometric area. A SEM picture taken at a magnification of 500 × is presented in Fig. 1.

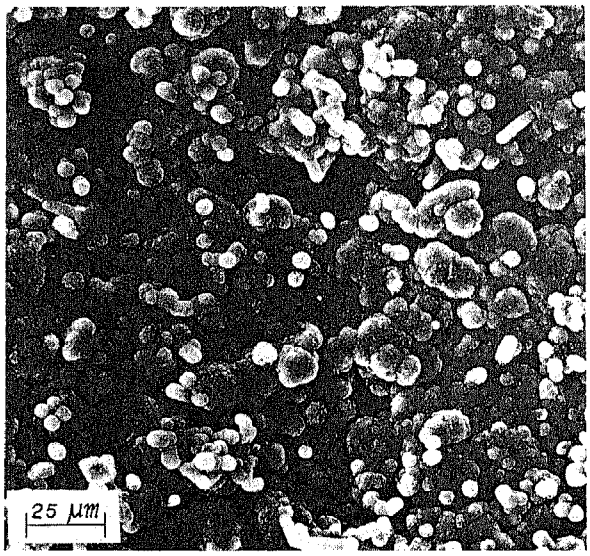

Fig. 1
Micrograph of polycrystalline BP deposited on alumina substrates

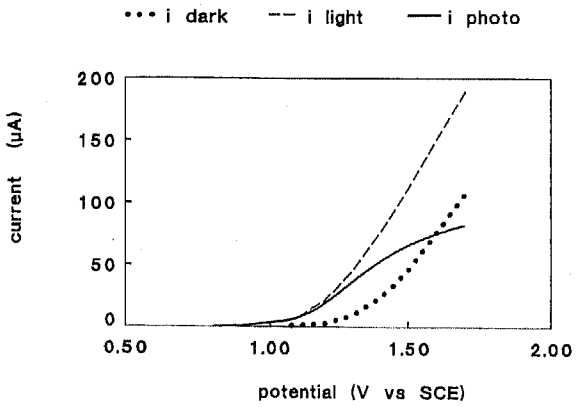

Fig. 2
(Photo-) Current-voltage characteristics of polycrystalline BP in H_2SO_4 (0.1 M). (1) dark-, (2) light-, (3) photocurrent

All samples exhibit n-type conductivity. Typical values for the resistivity, the donor density (N_D) and the Hall electron mobility are: 5 ohm-cm, 10^{19} cm^{-3}, and 0.13 cm^2/Vs, respectively.

Current-voltage curves reveal diode characteristics as is to be expected for Schottky barrier junctions. Upon illumination an anodic-, and in some cases a minor cathodic photocurrent is measured. The maximum observed anodic photocurrent in electrolyte 1 is about 0.5 mA/cm^2 which is very small with respect to the intensity of the incident radiation. The anodic photocurrent onset potential varies for the different samples between 0.1 and 0.5 V vs. SCE in electrolyte 1. Broad "S"-shaped photocurrent curves towards sat-

uration are observed. In Fig. 2 current-voltage curves are presented. In this figure the $i-V$ curves in the dark: i-dark vs. V, upon illumination i-light vs. V, and the photocurrent i-photo (= i-light minus i-dark) vs. V are shown. It is observed that whenever an anodic current is flowing, gas formation, presumably oxygen, occurs at the BP electrode surface.

Transient $i-V$ curves — recorded with chopped polychromatic illumination — clearly revealed a trapping effect. In a potential region positive to the photocurrent onset potential a fast anodic photocurrent overshoot was observed when the light was turned on. When switching off the light a similar but larger cathodic dark current overshoot was recorded. The overshoot duration is in the subsecond region whereas the photocurrent stabilizes not before 15 minutes. In Fig. 3 the transient photocurrent behavior is presented.

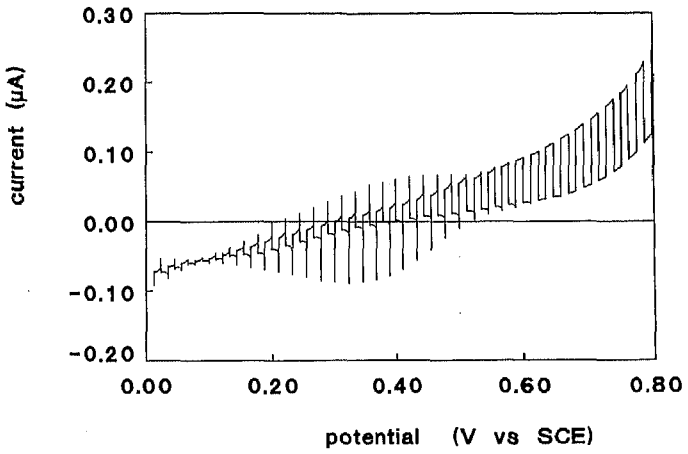

Fig. 3
Transient $i-V$ behavior obtained in H_2SO_4 (0.1 M) with chopped illumination: light on period 20 seconds/light off period 20 seconds. Scan direction is from positive to negative potentials

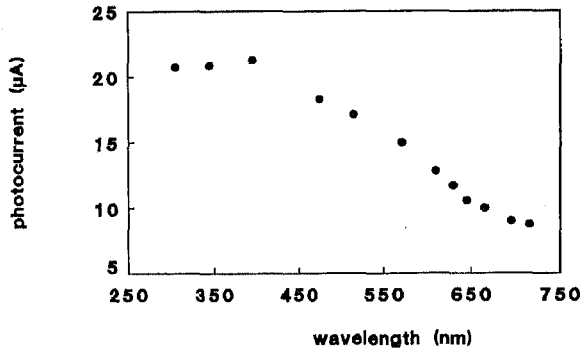

Fig. 4
Spectral dependence of the photocurrent in polycrystalline BP polarized at 1.2 V vs. SCE obtained with high pass filter glasses

The presence of electron states in the forbidden gap is also obvious from spectral photocurrents. In Fig. 4 it is clear that excitation with low energy photons $h\nu < E_g$, leads to noticeable photocurrents. Even at wavelengths larger than 715 nm, which is far beyond the 2.0 eV indirect bandgap at 620 nm, light is absorbed and results in free charge carriers. The presence of electron states within the forbidden zone is required to account for this subbandgap photocurrent.

The small-signal a.c. response of the PEC cell is represented as an admittance diagram in Fig. 5. In this figure, the imaginary component of the admittance, Y'', is plotted versus the real component, Y'.

Non linear least squares (NLLS) fitting to equivalent circuits yielded RW s C_{SC} p Q s R_F p R_S s C p, where p stands for parallel and s for series, to adequately model the PEC cell's small signal

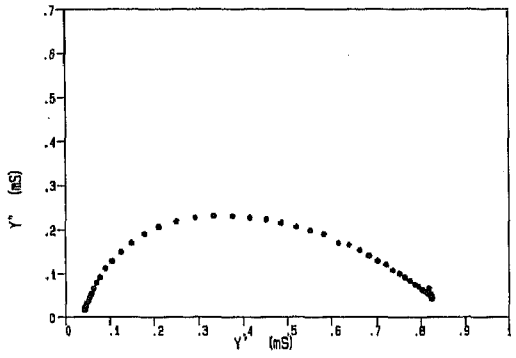

Fig. 5
Admittance diagram of Y'' vs. Y' in the frequency range 10^{-1} to 10^4 Hz of a polycrystalline BP electrode in H_2SO_4 (0.1 M) without illumination

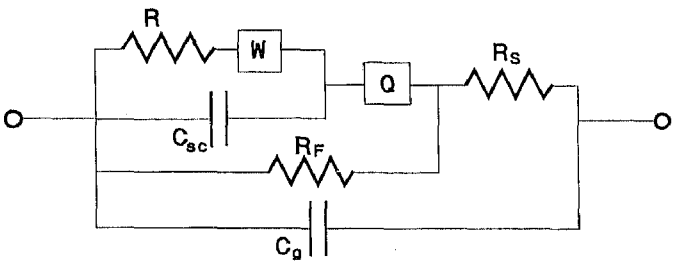

Fig. 6
Equivalent circuit which adequately model the small signal a.c. response of the system in the frequency range 10^{-1} to 10^4 Hz

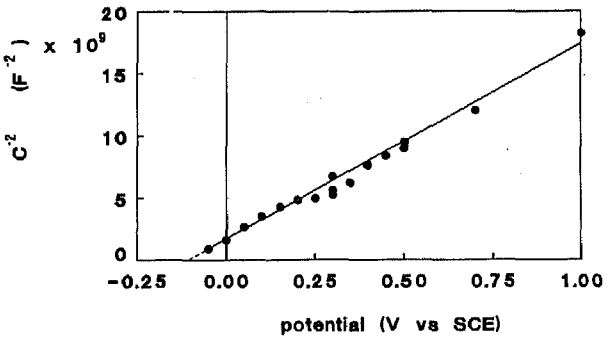

Fig. 7
Mott-Schottky plot of polycrystalline BP in the dark with H_2SO_4 (0.1 M) as electrolyte

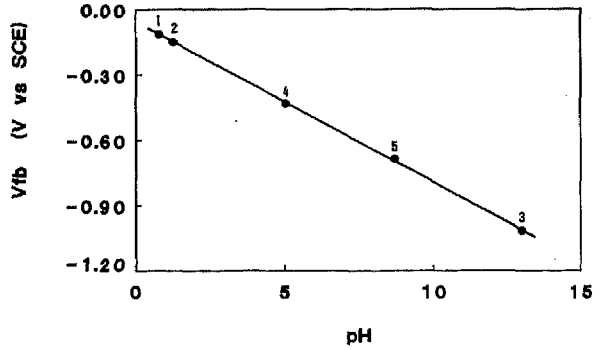

Fig. 8
pH dependence of the flatband potential. The numbers correspond with the various electrolytes: [1] H_2SO_4 (0.1 M), [2] H_2SO_4 (0.05 M) + KCl (1 M), [3] KOH (0.1 M), [4] HAc (0.05 M) + NaAc (0.05 M) + KCl (1 M), [5] KCl (1 M) + $Na_2B_4O_7$ (0.1 M)

a.c. response. Fig. 6 presents the equivalent circuit of the system under study in the dark. A survey of the results from fitting the model to the measured impedance data is presented in Table 1. In the reduced frequency range 0.1 to 10 Hz this complicated equivalent circuit can be simplified to R_F C_{SC} p R_S s to model the system's response with reasonable accuracy.

Table 1
The potential dependence of the equivalent circuit element parameters

V (V vs. SCE)	R_F (kΩ)	C_{SC} (μF)	R (kΩ)	W (μS $s^{1/2}$)
−0.05	25.4	33.4	25.3	73.1
0.0	28.8	25.0	43.4	25.1
0.05	62.8	19.5	52.8	17.5
0.1	46.7	16.9	24.4	30.8
0.15	79.3	15.3	32.0	30.0
0.2	102	14.4	36.9	29.5
0.25	146	14.2	35.0	27.8
0.3	∞	13.8	33.8	50.3
0.35	∞	12.7	41.1	47.8
0.4	∞	11.4	46.7	43.3
0.5	∞	10.5	54.4	61.4
0.7	∞	9.12	103	103
1.0	∞	7.41	122	47.5

R_S varies between 1.03 kΩ and 1.15 kΩ.
Q varies from 0.14 at 0.05 V to 0.37 mS s^{α} at −1.0 V vs. SCE.
α varies from 0.48 at 0.05 V to 0.33 at −1.0 V vs. SCE.
C_G is about 7 nF.

The data for the frequency independent space charge capacitance, C_{SC}, were used to construct the usual Mott-Schottky plots of C^{-2} versus V. In Fig. 7 this plot is shown for data recorded H_2SO_4 (0.1 M) having a pH of 1.24.

The flatband potential is observed to depend linearly on the electrolyte pH value. In Fig. 8 this dependence is presented.

The current-voltage characteristics as well as the impedance data recorded in the electrolytes 2 to 5 are qualitatively similar to the data presented above for electrolyte 1.

Discussion and Conclusions

Polycrystalline BP can be deposited onto alumina substrates by a conventional CVD process. When annealed the coatings exhibit the desired semiconducting properties and can serve as photoanode in a PEC cell.

All samples are n-type with low resistivity and a high donor density. Since no elements but B and P are present, the conduction in the layers is determined by an excess of P over B. Whether the excess P atoms are incorporated as interstitials or present as substitutional atoms has not been determined yet. Annealing the samples at 900°C removes part of the excess of P atoms and thus lowers the donor density. The magnitude of the resistivity as well as the donor density, as obtained with the Van der Pauw method, is sensitive to surface inhomogeneities and the microstructure of the semiconductor film [6]. With regard to the results in Fig. 1 grain boundary polarization phenomena cannot be ruled out in the present films. Hence the Van der Pauw resistivity may be too large, and the donor density too low.

The value of the dielectric constant (ε) of BP is reported to be 11 [7]. This value is obtained from Schottky barrier reflectance measurements applied to single crystals. Again inhomogeneities have not been taken into account.

Bringing BP into contact with an electrolyte leads to a Schottky barrier. The presence of this Schottky barrier makes it possible to obtain a photocurrent when illuminating the semiconductor surface. Current-voltage curves, as shown in Fig. 2, show the expected diode behavior. At low anodic polarization the current is blocked, but when increasing the polarization to values higher than about 1.2 V vs. SCE, the blocking capability of the heterojunction is lowered probably due to the presence of holes at the surface. At these voltages inversion occurs. We assume that the observed gas formation at the BP surface must be related to charge transfer processes between the BP valence band and the electrolyte. Hole capture from the valence band by the electrolyte results in the formation of oxygen. Apparently, charge transfer between the BP valence band and the electrolyte can compete strongly with either recombination processes or (photo-) anodic decomposition of the semiconductor.

Upon illumination, wide "S"-shaped photocurrent-voltage curves are obtained. The observed photocurrents are very small. At high anodic potentials a deviation from the maximum- or saturation photocurrent occurs. Effective electron/hole recombination seems to compete strongly with the charge transfer current even in this potential region. The width of the space charge layer (W) is defined as:

$$W = W_0\left(V - V_{fb} - \frac{kT}{e}\right)^{1/2} \quad \text{with} \quad W_0 \equiv \left(\frac{2\varepsilon\varepsilon_0}{eN_D}\right)^{1/2}.$$

Taking N_D to be 10^{19} cm^{-3} and ε to be 11, than W_0 is found to be about 11 nm. Boron phosphide is known to be a semiconductor with an indirect fundamental optical absorption with the absorption coefficient, a, ranging between 13 cm^{-1} at λ = 700 nm and 190 cm^{-1} at λ = 400 nm [8]. Since the product $W \times a$ is much smaller than 1, the major part of the incoming photons is absorbed far outside the space charge region in the bulk of the semiconductor. The Hall mobility of the majority charge carriers is observed to be very small in this polycrystalline material and this is likely to apply for the minority carrier mobility as well. Since the mean free path will be very small, diffusion of photocreated holes in the bulk of the semiconductor can cause hole transport towards the depletion region only across very small distances and thus cannot contribute to the photocurrent to a large extent. Taking the high donor density and the small mobility into account, it is obvious that most of the photo-electrons and photo-holes are created far outside the depletion region and cannot reach this region by diffusion due to fast bulk recombination processes. Only an amount of about $W \times a$ (≈0.02% at 400 nm excitation) of the photoholes can reach the semiconductor surface and may take part in a redox reaction — and thus contribute to the photocurrent — if surface recombination is absent. A very low quantum efficiency defined as i-photo/Φ^0 (with Φ^0 the intensity of the incoming light) must, therefore, be expected.

From transient photocurrent experiments, using chopped illumination, presented in Fig. 3, effective trapping and recombination via intragap states is obvious. The photocurrent- and the dark current overshoot can be ascribed to

charging and discharging of intragap states. When turning the light on, holes are created and are used to occupy intragap states until a steady state hole occupation is reached. This process causes an anodic transient current spike. When switching off the light, the hole density at the surface, and thus the hole capture rate, is reduced and electrons from the conduction band are able to empty the states until a new steady state occupation is reached. This process is responsible for a cathodic current spike. The time constant observed in the charging/discharging process of the intragap states is in the millisecond region which is rather long. In order to explain this slow trapping and recombination, two models will be discussed briefly.

First it is possible that the trapping and recombination occurs via states which are present either in the space charge region or at the surface of the semiconductor. A small state density results in slow recombination processes since the time constant for recombination via intragap states is linear in the reciprocal of the state density. The nature of polycrystalline semiconductors does not seem to justify a small intragap state density though.

A second model is derived from the assumption that a chemical reaction is involved in the trapping and recombination process. In this case the intragap electronic states are not present in the semiconductor, but in the electrolyte. In fact, Parent et al. [9] performed similar transient experiments on Fe_2O_3. They observed large transient current spikes compared to the steady state current in the photoanodic regime of the $i-V$ curve. Similar to our results this transient behavior is present under low applied anodic potentials, goes through a maximum, and disappears at more positive potentials. This behavior has been described by Iwanski et al. [10] to photogenerated holes which produce either an intermediate species in the water oxidation (or oxygen), or the oxidized species (Ox) of a redox couple. In addition to the photogenerated holes, electrons from the conduction band are suggested to be able to reach the semiconductor surface. A large density of electron states within the forbidden zone in the space charge region may cause electron transport to the surface under depletion conditions. Surface electrons would be able to reduce the oxidized species in the electrolyte which were produced earlier by the photogenerated holes, hence a cathodic back reaction is set on immediately after the anodic reaction is started. When switching off the light a cathodic back reaction will continue until the oxidized species in the electrolyte near the semiconductor surface are used in the redox reaction.

The nature of the recombination processes, responsible for the observed effects in boron phosphide electrodes, are still not fully understood.

The existence of a photocurrent at low energy subbandgap excitation also suggests the presence of a large density of trap states in the semiconductor space charge region. Electrons in such trap states can be excited to the conduction band, or holes to the valence band, under the absorption of subbandgap photons leading to a noticeable photocurrent.

Impedance spectroscopy revealed a spectrum which could be modelled with the equivalent circuit of Fig. 5. Each element in the equivalent circuit is assumed to correspond with an electrochemical process in the system under study. Here the equivalent circuit is build up of seven elements. Although we will focus on one of these elements only i.e. the space charge capacitance, a brief discussion of the nature of the other elements is given:

- R_S resistance due to both ohmic losses in the electrolyte $<100\ \Omega$, and the semiconductor bulk resistance.
- C_G geometric capacitance, possibly caused by the reference electrode.
- R_F Faradaic resistance, i.e. the d.c. conduction path across the space charge region in the semiconductor.
- C_{SC} semiconductor space charge capacitance.
- Q non Debye element with impedance: $Z = Q^{-1}(j\omega)^{-\alpha}$ which is associated to inhomogeneous diffusion of ions in the electrolyte towards the rough semiconductor surface, together (in series) with the diffusion of electrons through the semiconducting layer towards the four ohmic contacts.
- W Warburg impedance: $Z = W^{-1}(j\omega)^{-1/2}$ which is associated with diffusion in the space charge region of electrons or holes.
- R ohmic losses in the semiconductor space charge region, related to electron or hole migration.

Fig. 7 shows a linear relation between C^{-2} and V. Apparently the space charge capacitance obeys the Mott-Schottky relationship:

$$C_{SC}^{-2} = \frac{2}{\varepsilon\varepsilon_0 e N_D A^2}\left(\Delta V_{SC} - \frac{kT}{e}\right).$$

In this expression ΔV_{sc} is the potential drop across the semiconductor under depletion. When the additional potential drop across the Helmholtz double layer can be neglected ΔV_{sc} can be set equal to $V - V_{fb}$. In this case linear and frequency independent Mott-Schottky plots, of C^{-2} vs. V, can be used to obtain the flatband potential. From the slope of the plot, the product $N_D \times A^2$ can be calculated which will yield a value for N_D if A is known. The flatband potential of polycrystalline BP, appears to be $(-0.060-0.073\ \text{pH})$ V vs. SCE. Versus the standard hydrogen potential: V_{fb} is $(+0.182-0.073\ \text{pH})$ V. In these values, a correction for a possible potential drop across the Helmholtz double layer has not been taken into account. Estimating the conduction band to be positioned at 0.1 eV above the Fermi level, which is confirmed by the temperature dependence of the thermoelectric power (Seebeck effect), and taking a bandgap value of 2.0 eV it can be concluded that the position of the conduction band, and the valence band at pH = 0 is at 0.082 and 2.082 V vs. SHE, respectively. Using atomic electronegativities Butler and Ginley were able to obtain an expression for the position of the flatband potential [4, 11]. To apply this model to BP the values for the atomic electron affinity and for the first excitation energy for B and P are required. The atomic electronegativity, defined as the mean value of the electron affinity and the first ionization energy, is for B: $\chi = 4.290$ eV and for P: $\chi = 5.615$ eV [12]. The molecular electronegativity is a proportional mean value of the atomic electronegativities and is found to be 4.91 eV for

BP. This molecular electronegativity is assumed to be identical to the position of the Fermi level in the intrinsic semiconductor. In general, this position is halfway the forbidden zone. Assuming the position of the Fermi level in extrinsic BP to be positioned at about 0.1 eV below the conduction band, a value of -0.49 V vs. SHE for the position of the Fermi level is found. In the ideal case the extrinsic Fermi level position coincides with the flatband potential. Comparing the calculated flatband potential of -0.5 V vs. SHE to the experimentally determined value a discrepancy is noticed. This discrepancy may be caused by the additional potential drop in the Helmholtz layer due to specifically adsorbed species from the electrolyte at the semiconductor surface or due to accumulated charge in semiconductor surface states. Only when the net absorbed charge at the surface is zero the experimentally determined flatband potential can be compared with the calculated value. At a pH of about 9.3 the experimental and calculated values are equal. Therefore, the point were no net charge is absorbed, "point of zero zeta potential", is found at pH = 9.3. This value is rather high, but not unrealistic.

Compared with the well known 111-V semiconductors: GaP, GaAs, and InP, with their conduction band energies at pH = 0 of: +1.05, +0.9, and +0.25 eV vs. SHE, respectively [13], the conduction band energy of BP which is -0.082 eV vs. SHE is surprisingly low.

The BP valence band is positioned at a higher potential than the H_2O/O_2 redox potential. Consequently photocreated holes in BP are able to oxidize H_2O to O_2. This feature makes BP a candidate anode material in a cell for photoelectrolysis of water. Oxygen formation at an illuminated BP anode has indeed been observed in our study.

The flatband potential of BP is noticed to depend on the electrolyte pH in a linear way between pH 0 and pH 14 as is presented in Fig. 8. This observation strongly suggests that the BP surface in aqueous electrolyte solutions contains hydroxide groups which are more or less in acid-base equilibrium with the solution. In GaAs, GaP [13] and in InP [14] a similar pH dependence is reported. In GaAs and GaP a Nernstein behavior is found [13] but in InP there appeared to be a non-linear pH dependence [14].

When the donor density is calculated from the slope of the Mott-Schottky plots, substituting a value of 0.2 cm^2 for the surface area, A, a donor density of 3.3×10^{21} cm^{-3} is obtained. This number can be compared with the donor density obtained from Hall potentials being 10^{19} cm^{-3}. A difference of more than two orders of magnitude is found between these two independent methods. The roughness of the electrode surface as is shown in Fig. 1 can be responsible for this clear discrepancy. The space charge layer is able to follow the curvature of the surface on a submicron scale. Obviously a large deviation between the geometrical surface area and the surface area as been measured on a submicron scale occurs. Assuming the Hall donor density to be accurate we are able to calculate the ratio between the "real" electrolyte/semiconductor contact area, and the geometric area. In this case a ratio of 18 is found.

We are grateful to Dr. D. Vanmaekelbergh and Prof. Dr. J. J. Kelly for their encouraging interest and their helpful advises in this study. We also would like to express our gratitude to Ir. R. Hofman and Dr. Ir. J. Schram for experimental assistance and fruitful discussions.

The investigations were supported by the Netherlands Foundation for Chemical Research (SON) with financial aid from the Netherlands Organization for Scientific Research (NWO).

References

[1] Landolt-Börnstein, Band 3/17a. p. 153, Springer-Verlag, Berlin 1982.
[2] K. Shono, H. Othako, and J. Bloem, J. Cryst. Growth *45*, 187 (1978).
[3] T. Takenaka, M. Takigawa, and K. Shohno, J. Electrochem. Soc. *125*, 633 (1978).
[4] D. S. Ginley, R. J. Baughman, and M. A. Butler, J. Electrochem. Soc. *130*, 1999 (1983).
[5] M. A. Butler and D. S. Ginley, J. Electrochem. Soc. *125*, 228 (1978).
[6] L. J. van der Pauw, Philips Res. Rep. *13*, 1 (1958).
[7] T. Takenaka, M. Takigawa, and K. Shohno, Jpn. J. Appl. Phys. *15*, 2021 (1976).
[8] R. J. Archer, R. Y. Koyama, E. E. Loebner, and R. C. Lucas, Phys. Rev. Lett. *12*, 538 (1964).
[9] L. Parent, J. P. Dodelet, and S. Dallaire, J. Electrochem. Soc. *134*, 2226 (1987).
[10] P. Iwanski, J. S. Curran, W. Gissler, and R. Memming, J. Electrochem. Soc. *128*, 2128 (1981).
[11] M. A. Butler and D. S. Ginley, Chem. Phys. Lett. *47*, 319 (1977).
[12] Lange's Handbook of Chemistry, McGraw Hill Book Company, 12th edition 1979.
[13] W. P. Gomes and F. Cardon, Progr. Surf. Sci. *2*, 155 (1982).
[14] M. van Wezemael, W. H. Laflere, and F. Cardon, J. Electroanal. Chem. *87*, 105 (1978).

(Eingegangen am 20. Februar 1989, endgültige Fassung am 12. Juni 1989) E 7018